International Journal of Applied Mathematics in Control Engineering 2 (2018) 187-193

Contents lists available at YXpublications

International Journal of Applied Mathematics in Control Engineering

Journal homepage: http://www.ijamce.com

Back-stepping Sliding Mode with Unidirectional Auxiliary Surfaces for HSV with Attitude Constrains

Zhihao Yang[a,*], Jian Fu[a], Liangming Wang[a] , Zhi Chen[b] , Hongyang Bai[a]

[a] *School of Energy and Power Engineering, Nanjing University of Sciences and Technology, 210094, Nanjing*

[b] *School of Mechatronic Engineering and Automation, Shanghai University, 200072, Shanghai*

ARTICLE INFO

Article history:
Received 30 July 2018
Accepted 18 October 2018
Available online 25 December 2018

Keywords:
Hypersonic Vehicle
Sliding mode control
Nonlinear Control
Back-stepping

ABSTRACT

A special kind of back-stepping sliding mode control with unidirectional auxiliary surfaces (UAS-BSMC) method is proposed for HSV systems with attitude constraints in this paper. Based on the positively invariant sets, an innovative sliding surface is developed to guarantee the attitude constraints. Then the back-stepping control method is utilized to design the slow-loop and fast-loop controller. The convergence of all closed-loop signals is proved via Lyapunov analysis method under the control scheme. Simulation results are given to illustrate the benefits and properties of the proposed algorithm.

1. Introduction

Recently, hypersonic vehicle (HSV) has drawn people's attention. To fully utilize the special characterizations of HSV, it is necessary to develop an efficient control scheme which meets the requirements of flight system. Nowadays, lots of flight control algorithms have been applied to HSV, like the back-stepping control method (e.g., Shao X et al., 2016), sliding mode control method (e.g., Zhang Y et al., 2016), adaptive control method (e.g., Bu X et al., 2016), fault-tolerant control method (e.g., Xu B et al., 2016) and so on. Back-stepping control is known as a construction approach in the sense that it has a systematic way of constructing the Lyapunov function along with the control input design. In the process of backtracking, the parameters can be modified and the stability of the system can be improved by some methods, such as designing a series of filters or Lyapunov functions. Finally, the controller to make the original system stable is obtained (e.g., Y. Zhu et al., 2015). However, back-stepping control method is susceptible to disturbances (e.g., Yin C et al., 2018). Therefore, the sliding mode control method which is much more robust is used to enhance the stability of the system.

The sliding mode control (SMC) strategy has attracted considerable attention in the last two decades in both industrial and academic communities. Due to its high robust features and convenience for real implementation, this control scheme has been widely applied in many applications such as magnetic bearing systems (e.g., Shi S et al., 2018), speed controller of permanent magnet synchronous motor(e.g., Yan L et al., 2009), spacecraft (e.g., Pukdeboon C et al., 2009) and robots (e.g., Luo X et al., 2018). However, most of the SMC control methods for HSV have not considered the attitude constraints. Thus, it is necessary to design an innovative sliding mode control method for HSV with attitude constraints.

This work is motivated by the robust attitude control of HSV with attitude constraints. The control objective is to track a desired trajectory with attitude constraints. In this article, a technique called back-stepping sliding mode control with unidirectional auxiliary surfaces (UAS-BSMC) is presented to design positively invariant (PI) sets for the control design of HSV. The foundation of positively-invariant set Qi resulting in trajectories remaining in Qi for all subsequent times (e.g., Polyakov. et al., 2011).Unidirectional auxiliary surfaces, which naturally form PI sets, are utilized in this method. The main advantage of this design is that system states are constrained by unidirectional auxiliary surfaces instead of switching surfaces. Then, constraints are guaranteed when system states leaving the switching surfaces. Rigorous stability analysis is guaranteed with Lyapunov analysis which shows the asymptotical convergence of the closed-loop signals. And the structure of this paper is organized as follows: Problem statement is given in the

* Corresponding author.
E-mail addresses: zh.young@foxmail.com (Z. Yang)

following section. Next, the stability of the system and the positively invariant sets are proved in this paper. Simulation results show the effectiveness of this method. Last section concludes the paper.

2. Problem statement

The six-degree-of-freedom kinematic equations for an HSV are given by (e.g., Han Z et al., 2014):

$$\begin{cases} \dfrac{\mathrm{d}\gamma}{\mathrm{dt}} = \omega_x - \omega_z \tan\varphi_2 \\ \dfrac{\mathrm{d}\varphi_a}{\mathrm{dt}} = \dfrac{\omega_z}{\cos\varphi_2} \\ \dfrac{\mathrm{d}\varphi_2}{\mathrm{dt}} = -\omega_y \\ \dfrac{\mathrm{d}\omega_x}{\mathrm{d}t} = \dfrac{1}{C}\left(M_{xs} + M_{xc}\right) \\ \dfrac{\mathrm{d}\omega_y}{\mathrm{d}t} = \dfrac{1}{A}\left(M_{ys} + M_{yc}\right) - \dfrac{C}{A}\omega_z\omega_x + \omega_z^{\ 2}\tan\varphi_2 \\ \dfrac{\mathrm{d}\omega_z}{\mathrm{d}t} = \dfrac{1}{A}\left(M_{zs} + M_{zc}\right) - \omega_y\omega_z \tan\varphi_2 + \dfrac{C}{A}\omega_y\omega_x \end{cases} \tag{1}$$

where $x_1 = [\gamma, \varphi_a, \varphi_2]^{\mathrm{T}} \in R^3$ is the attitude angle vector of slow-loop states, $x_2 = [\omega_x, \omega_y, \omega_z] \in R^3$ is the body axis angular rate vector of fast-loop states. C is the moment of inertia through the x-axis, A is the moment of inertia through the y-axis. $u = [M_{xc}, M_{yc}, M_{zc}] \in R^3$ is the vector of control moments consisting of roll, pitching, and yaw control moments. $u = [M_{xs}, M_{ys}, M_{zs}] \in R^3$ is the vector of other states moments consisting of roll, pitching, and yaw control moments.

With the time-scale separation principle, the above attitude motion equations can be rewritten as follows

$$\begin{aligned} \dot{x}_1 &= f_1(x_1) + g_1(x_1)x_2 \\ \dot{x}_2 &= f_2(x_1, x_2) + g_2(x_1, x_2)u \end{aligned} \tag{2}$$

During the hypersonic phase, HSV is usually sensitive to the changes of attitude angles (e.g., Walton J. et al., 2002). Thus, attitude constraints are necessary to guarantee the performance of HSV. In this article, the control objective is to design the robust UAS-SMC controller which efficiently tracks a given desired attitude motion $y_d = [y_{d1}, y_{d2}, y_{d3}]^{\mathrm{T}}$ in the presence of attitude constraints.

Assumption 1. The generalized matrix inverses of $g_1(x_1)$ and $g_2(x_1, x_2)$ are always existing for the nonlinear attitude motion model of the HSV.

Remark 1. Actually, Assumption 1 is always satisfied from the detailed definitions (e.g., Fu J et al., 2013).

Assumption 2. The elements in matrixes $f_1(x_1), g_1(x_1)$, $f_2(x_1, x_2), g_2(x_1, x_2)$ are always continuous for the nonlinear attitude motion model of the HSV.

3. Robust attitude control with attitude constraints

In this section, we consider the robust attitude control for HSV systems (1) with attitude constraints. UAS-BSMC method is used to design the controller for the attitude constraints, for simplicity, define

$$\begin{aligned} e_1 &= x_1 - y_d \\ e_2 &= x_2 - \nu_1 \end{aligned} \tag{3}$$

where $\nu_1 \in R^3$ is a designed virtual control law. Then, considering equation (1), the derivatives $\dot{e}_1, \dot{e}_2$ can be written as

$$\begin{aligned} \dot{e}_1 &= f_1(x_1) + g_1(x_1)(e_2 + \nu_1) - \dot{y}_d \\ \dot{e}_2 &= f_2(x_1, x_2) + g_2(x_1, x_2)u - \dot{\nu}_1 \end{aligned} \tag{4}$$

$e_1 = [e_{11}, e_{12}, e_{13}]^{\mathrm{T}} \in R^3$ are the state errors of slow-loop states, $e_2 = [e_{21}, e_{22}, e_{23}]^{\mathrm{T}} \in R^3$ are the state errors of fast-loop states. The attitude constraints can be rewritten as

$$\psi = \left\{ \left(e_1, \int e_1\right) \middle| -c_i \le e_{1i} \le c_i \right\} \quad c_i \in R^+, i = 1,2,3 \tag{5}$$

where $\psi = [\psi_1, \psi_2, \psi_3]^T$,and $\psi_i = \left\{ \left(e_{1i}, \int e_{1i}\right) \middle| -c_i \le e_{1i} \le c_i \right\}$.

Assumption 3. For all $t > 0$, there exists e_{1i} which satisfies the constraints (5).

Definition 1. (e.g., Blanchini F et al., 2002) The set Q is said positively invariant (PI) for nonlinear system (2), if for all $x_1(0) \in Q$, the solution $x_1(t) \in Q, \forall t > 0$.

Assumption 4. The initial state error $e_{1i}(0), i = 1,2,3$ is located in Q_{1i} where Q_{1i} is the designed PI set in section "Slow-loop UAS-SMC controller design".

3.1 Slow-loop controller design

In this section, we address the PI sets for the constraints with UAS-BSMC method. The detailed design process is appended as follows.

Step 1. Considering the slow-loop in system (1), the switching surfaces S_{11} and S_{12} , are chosen as follows

$$\begin{cases} S_{11} = e_1 + \xi_{11}\int e_1 = 0 \\ S_{12} = e_1 + \xi_{12}\int e_1 = 0 \end{cases} \tag{6}$$

where

$$\begin{aligned} \xi_{11} &= diag\left\{\xi_{111}, \xi_{112}, \xi_{113}\right\} \\ \xi_{12} &= diag\left\{\xi_{121}, \xi_{122}, \xi_{123}\right\} \\ S_{11} &= \left[S_{111}, S_{112}, S_{113}\right]^T \\ S_{12} &= \left[S_{121}, S_{122}, S_{123}\right]^T \end{aligned}$$

$\xi_{11i} > \xi_{12i} > 0$, $i = 1,2,3.$ $\int e_1 dt$ is denoted by $\int e_1$ for the sake of brevity. Conditions $\xi_{11i} > 0$, $\xi_{12i} > 0$ is given to guarantee the stability of switching surface $S_{11i}=0$, $S_{12i}=0$. And condition $\xi_{11i}>0$, $\xi_{12i}>0$ is used to avoid the overlap of switching surfaces $S_{11i}=0$, $S_{12i}=0$.

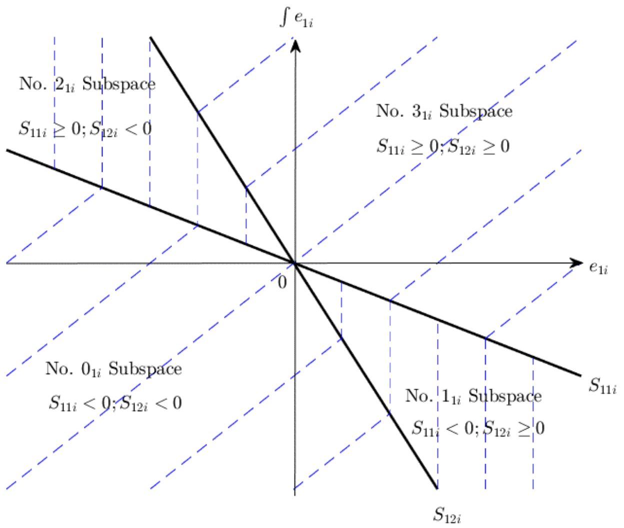

Fig. 1. The switching surfaces dividing the state space into four subspaces.

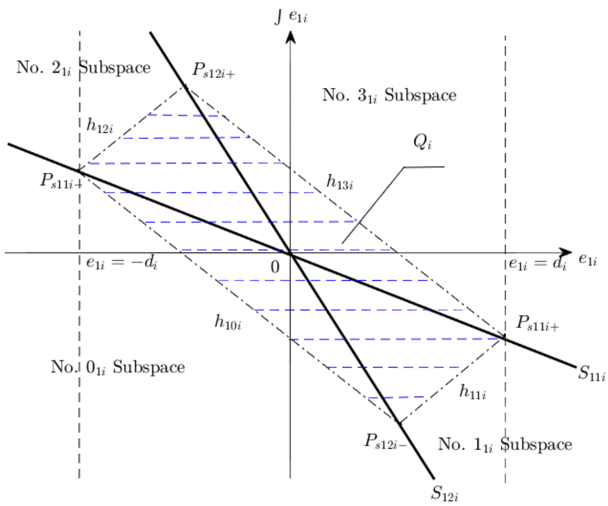

Fig. 2. The auxiliary surfaces and subsystems.

Step 2. As shown in Fig. 2, the appropriate points $P_{S11+}, P_{S11-}, P_{S12+}, P_{S12-}$ should be selected on switching surfaces $S_{11i}=0$, $S_{12i}=0$, where points P_{S11+}, P_{S12-} are located in the fourth quadrant and points P_{S11-}, P_{S12+} are located in the second quadrant. Then, the lines $P_{S11-}P_{S12-}$, $P_{S11+}P_{S12-}$, $P_{S11-}P_{S12+}$, $P_{S11+}P_{S12+}$ in Fig. 2 are defined as UAS $h_{10i}, h_{11i}, h_{12i}, h_{13i}$ respectively.

The formulas for these UAS are given as follows

$$h_{1ki}=\omega_{1ki1}x_i+\omega_{1ki2}\int x_i+m_{1i} \tag{7}$$

where $k\in\{0,1,2,3\}$, m_{1i} is a positive constant.

Step 3. The UAS in Fig. 2 would be utilized to design virtual control law v_1 when the states are moving in $No.0_{1i},1_{1i},2_{1i},3_{1i}$ Subspaces. The current UAS for state error e_{1i} is given as:

$$h_{1i}=\omega_{1i1}e_{1i}+\omega_{1i2}\int e_{1i}+m_{1i} \tag{8}$$

where

$$\omega_{1i1}=\begin{cases}\omega_{10i1} & s_{11i}<0, s_{12i}<0\\ \omega_{11i1} & s_{11i}<0, s_{12i}\geq 0\\ \omega_{12i1} & s_{11i}\geq 0, s_{12i}<0\\ \omega_{13i1} & s_{11i}\geq 0, s_{12i}\geq 0\end{cases},$$

$$\omega_{1i2}=\begin{cases}\omega_{10i2} & s_{11i}<0, s_{12i}<0\\ \omega_{11i2} & s_{11i}<0, s_{12i}\geq 0\\ \omega_{12i2} & s_{11i}\geq 0, s_{12i}<0\\ \omega_{13i2} & s_{11i}\geq 0, s_{12i}\geq 0\end{cases}$$

Consequently, a compact form of current UAS can be rewritten as

$$h_1=\Omega_{11}e_1+\Omega_{12}\int e_1+m_1 \tag{9}$$

where

$$\begin{aligned}h_1&=[h_{11},h_{12},h_{13}]^T\\ e_1&=[e_{11},e_{12},e_{13}]^T\\ \int e_1&=\left[\int e_{11},\int e_{12},\int e_{13}\right]^T\\ \Omega_{11}&=diag\{\omega_{111},\omega_{121},\omega_{131}\}\\ \Omega_{12}&=diag\{\omega_{112},\omega_{122},\omega_{132}\}\\ m&=[m_{11},m_{12},m_{13}]^T\end{aligned}$$

m is a positive constant vector.

As shown in Figure 2, the UAS surfaces can form a convex set Q_{1i} and the expression of the set Q_{1i} is written as

$$Q_{1i}=\left\{\left(e_{1i},\int e_{1i}\right)\middle| h_{1i}\geq 0\right\} \tag{10}$$

The compact form of convex set Q_{1i} can be written as $Q_1=[Q_{11},Q_{12},Q_{13}]^T$,where $Q_1\in\psi$ implies $Q_{1i}\in\psi_i$, $i=1,2,3$.

Step 4. The virtual control law v_1 for nonlinear system is designed as

$$v_1=g_1^{-1}\left(-f_1+\dot{y}_d-\Omega_{11}^{-1}\Omega_{12}e_1+\Omega_{11}^{-1}N_1\right) \tag{11}$$

where $N_1=[N_{11},N_{12},N_{13}]^T$ is the designed approaching law, $N_{1i}>0, i=1,2,3$.

Remark 2. The approaching law in traditional SMC method is often designed as

$$\dot{S}=-K\cdot sign(S),\ K>0 \tag{12}$$

$sign(\bullet)$ is a discontinuous sign function. From (12), $sign(S)$ can be positive or negative according to the $sign(S)$. We can say the direction of S is bidirectional in the traditional SMC method. On the other hand, there exists $\dot{h}(u)=N>0$ in UAS-BSMC method. Then, the direction of auxiliary surface h is unidirectional. That is why h is called unidirectional auxiliary surface in this paper.

Remark 3. It is noted that the derivative of virtual control laws v_1 is used in the controller (11) for HSV system (1). Assistant filters are introduced to obtain the derivatives of v_1, which avoids the spikes from differentiation in back-stepping control method. For brevity, the detailed design process is omitted here.

Invoking equation (1), (8), and (11), it is obtained that

$$\begin{aligned} \dot{h}_1 &= \Omega_{11}\dot{e}_1 + \Omega_{12}e_1 \\ &= \Omega_{11}\left(f_1 + g_1\left(e_2 + v_1\right) - \dot{y}_d\right) + \Omega_{12}e_1 \\ &= N_1 + \Omega_{11}g_1 e_2 \end{aligned} \tag{13}$$

Remark 4. The set $\{e_{1i} \mid h_{1i} \ge 0\}$ in Fig. 2 can be proved as a positively invariant set with UAS-BSMC controller. Thus, the UAS-BSMC method also can be called back-stepping sliding mode control with positively invariant set (PIS-BSMC) method.

3.2 Fast-loop controller design

In this section, robust sliding mode controller for the fast-loop system is designed by UAS-BSMC method.

Step 1. Considering the fast-loop in system (1), we define the switching surfaces as

$$\begin{cases} S_{12} = e_2 + \xi_{21}\int e_2 = 0 \\ S_{22} = e_2 + \xi_{22}\int e_2 = 0 \end{cases} \tag{14}$$

where $\xi_{11} = diag\{\xi_{111}, \xi_{112}, \xi_{113}\}$, $\xi_{12} = diag\{\xi_{121}, \xi_{122}, \xi_{123}\}$, $S_{11} = [S_{111}, S_{112}, S_{113}]^T$, $S_{12} = [S_{121}, S_{122}, S_{123}]^T$, $\xi_{11i} > \xi_{12i} > 0$, $i = 1, 2, 3$.

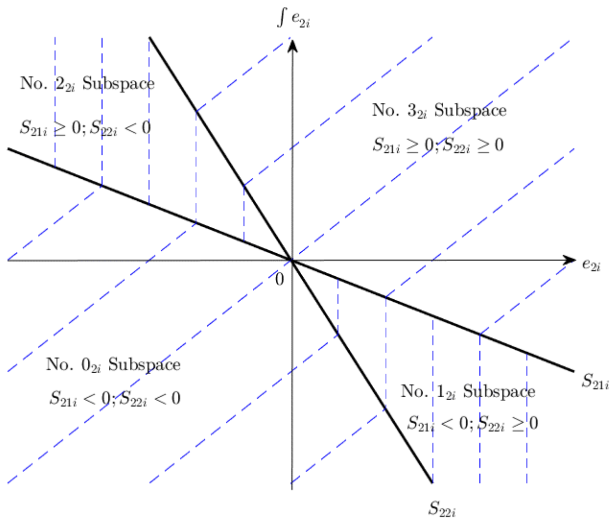

Fig. 3. The switching surfaces dividing the state space into four subspaces.

Step 2. As shown in Figure 3, the $No.0_{2i}, 1_{2i}, 2_{2i}, 3_{2i}$ subspaces are defined with switching surfaces S_{21i} and S_{22i}. Then, we can also design the UAS $h_{20i}, h_{21i}, h_{22i}, h_{23i}$ following Step 2 in the previous section.

$$h_{2ki} = \omega_{2ki1}x_i + \omega_{2ki2}\int x_i + m_{2i} \tag{15}$$

where $k \in \{0,1,2,3\}$, m_{1i} is a positive constant.

Step 3. Invoking equation (16), the current UAS is given as:

$$h_{2i} = \omega_{2i1}e_{2i} + \omega_{2i2}\int e_{2i} + m_{2i} \tag{16}$$

where

$$\omega_{i1} = \begin{cases} \omega_{20i1} & s_{21i} < 0, s_{22i} < 0 \\ \omega_{21i1} & s_{21i} < 0, s_{22i} \ge 0 \\ \omega_{22i1} & s_{21i} \ge 0, s_{22i} < 0 \\ \omega_{23i1} & s_{21i} \ge 0, s_{22i} \ge 0 \end{cases},$$

$$\omega_{i2} = \begin{cases} \omega_{20i2} & s_{21i} < 0, s_{22i} < 0 \\ \omega_{21i2} & s_{21i} < 0, s_{22i} \ge 0 \\ \omega_{22i2} & s_{21i} \ge 0, s_{22i} < 0 \\ \omega_{23i2} & s_{21i} \ge 0, s_{22i} \ge 0 \end{cases}$$

Consequently, a compact form of current UAS can be rewritten as

$$h_2 = \Omega_{21}e_2 + \Omega_{22}\int e_2 + m_2 \tag{17}$$

where

$$\begin{aligned} h_2 &= [h_{21}, h_{22}, h_{23}]^T \\ e_2 &= [e_{21}, e_{22}, e_{23}]^T \\ \int e_1 &= \left[\int e_{21}, \int e_{22}, \int e_{23}\right]^T \\ \Omega_{21} &= diag\{\omega_{211}, \omega_{221}, \omega_{231}\} \\ \Omega_{22} &= diag\{\omega_{212}, \omega_{222}, \omega_{232}\} \\ m &= [m_{21}, m_{22}, m_{23}]^T \end{aligned}$$

Step 4. Invoking equation (19), the UAS-BSMC controller for the fast-loop system (2) is given as

$$u = g_2^{-1}\left(-f_2 + \dot{v}_1 + \Omega_{21}^{-1}N_2 - \Omega_{21}^{-1}\Omega_{11}g_1 e_2 - \Omega_{21}^{-1}\Omega_{22}e_2\right) \tag{18}$$

Step 5. Defining $E^T = [1,1,1]^T$, for considering the stability of states for the closed control system, the Lyapunov function candidate is chosen as

$$V = E^T\left(m_1 - h_1\right) + E^T\left(m_2 - h_2\right) \tag{19}$$

It is noted that Lyapunov function candidate V is a continuous function for all $e \in R^3$ (e.g., Fu J et al., 2013).

The time derivative of V is invoking equations (11), (16), (18), and (19), the time derivative is

$$\begin{aligned} \dot{V} &= E^T\left(-\Omega_{11}\dot{e}_1 - \Omega_{12}e_1\right) + E^T\left(-\Omega_{21}\dot{e}_2 - \Omega_{22}e_2\right) \\ &= -E^T N_1 - E^T\Omega_{11}g_1 e_2 \\ &\quad - E^T\Omega_{21}\left(f_2 + g_2 u - \dot{v}_1\right) - E^T\Omega_{22}e_2 \\ &= -E^T N_1 - E^T N_2 \\ &< 0 \end{aligned} \tag{20}$$

Thus, the system (2) is asymptotically stable under the control law.

4. Results

In this section, simulation results are given to illustrate the effectiveness of the proposed adaptive UAS-BSMC schemes for HSV with attitude constraints. Suppose that the HSV vehicle lies in the cruise flight phase with the velocity 1700m/s and flight altitude 5 km. The initial attitude and attitude angular velocity conditions are chosen as

$$\gamma=0\deg,\ \ \varphi_a=0\deg,\ \ \varphi_2=0\deg$$

$$\omega_\xi=0\deg/s\quad \omega_\eta=0\deg/s\quad \omega_\zeta=0\deg/s\,.$$

The attitude constraints for the state error

$$\mathrm{e}_1=y-y_d=\left[e_1,e_2,e_3\right]^{\mathrm{T}}$$

are given as

$$\begin{aligned}-0.1^\circ &\le e_{11}\le 0.1^\circ\\ -0.02^\circ &\le e_{12}\le 0.02^\circ\\ -0.1^\circ &\le e_{13}\le 0.1^\circ\end{aligned}\tag{21}$$

The UAS-BSMC approaching laws N for HSV is designed as

$$N=\dot{h}=k\cdot\left(m-h\right)^{\alpha},k=2,\alpha=0.5\tag{22}$$

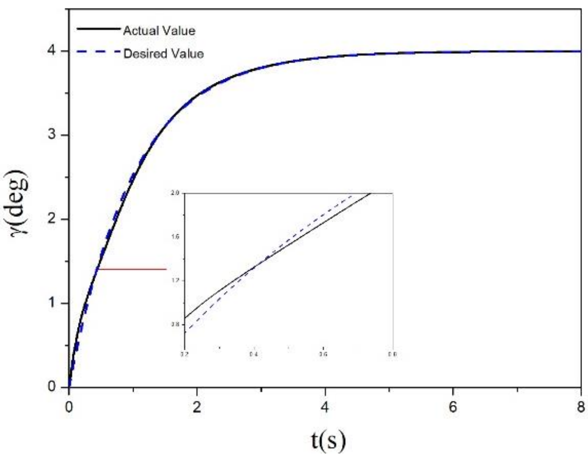

Fig. 4. The attitude responses γ under UAS-BSMC

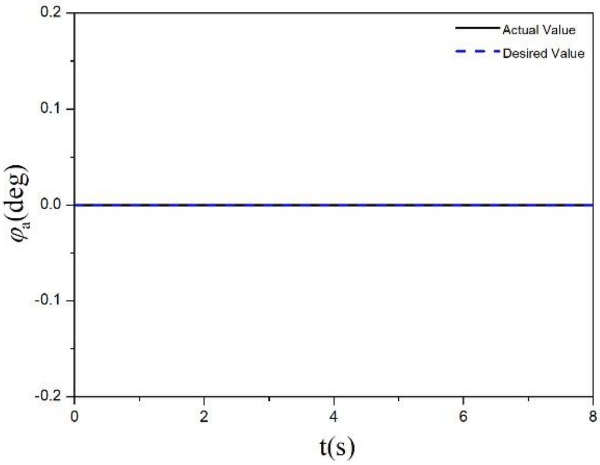

Fig. 5. The attitude responses φ_a under UAS-BSMC

In the simulation, we assume that the unknown time-varying disturbance moments imposed on the HSV are

$$\begin{aligned}d_{mx}\left(t\right)&=10\%\cdot M_{xs}\cdot\sin\left(\pi t\right)\\ d_{my}\left(t\right)&=10\%\cdot M_{ys}\cdot\sin\left(\pi t\right)\\ d_{mz}\left(t\right)&=10\%\cdot M_{zs}\cdot\sin\left(\pi t\right)\end{aligned}\tag{23}$$

The attitude responses are shown in Fig. 4 to Fig. 6

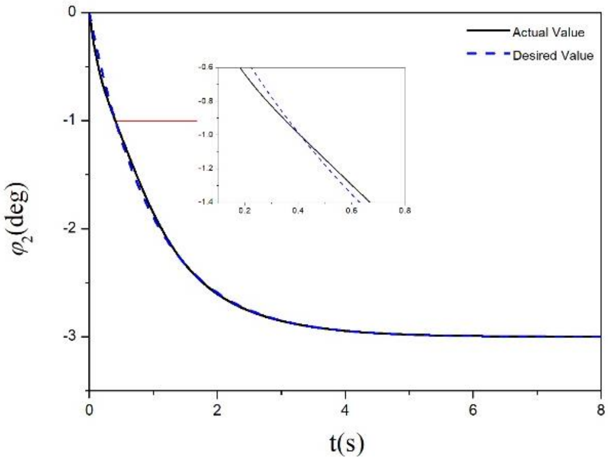

Fig. 6. The attitude responses φ_2 under UAS-BSMC

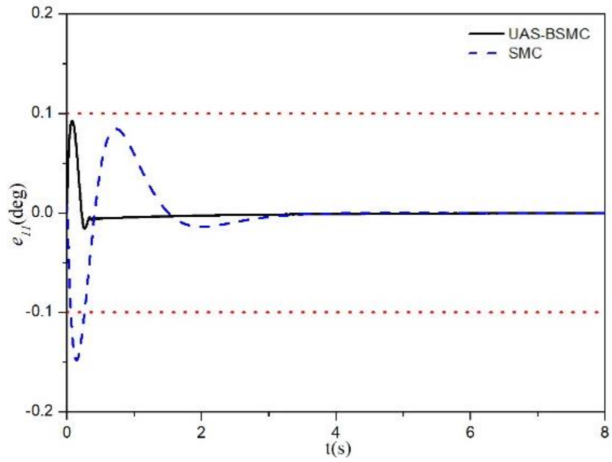

Fig. 7. The state error e_{11} under sliding mode and UAS-BSMC methods.

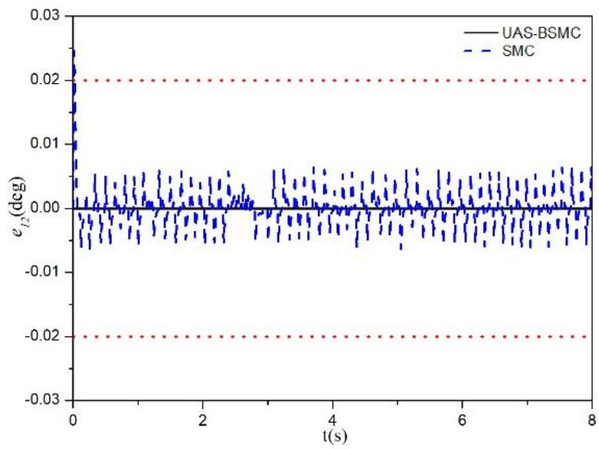

Fig. 8. The state error e_{12} under sliding mode and UAS-BSMC methods.

The simulation results of the HSV attitude flight control under designed controller are shown in Fig. 4 to Fig. 6. It can be seen form figure that the attitude angles output can quickly track the desired trajectory y_d.

To compare with the UAS-BSMC controller, we also design a traditional SMC controller for HSV. The switching surface S is defined as

$$\dot{S} = -k \cdot |S|^{\alpha} \, sign(S), \quad k = 2, \alpha = 0.5 \tag{24}$$

The state error responses are shown in Fig. 7 to Fig. 9 under SMC and UAS-BSMC methods respectively.

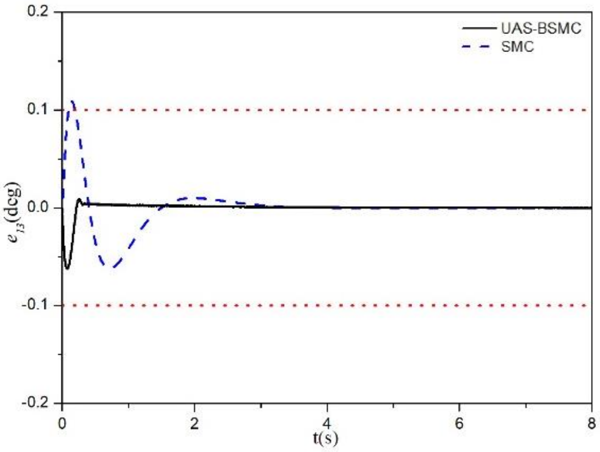

Fig. 9. The state error e_{13} under sliding mode and UAS-BSMC methods

Since the attitude constraints are not considered in the design process of SMC scheme, the undesirable overshoots are often found with inappropriate approaching laws. And these overshoots are harmful for the HSV system because they might be out of the attitude constraints (21). From the state error responses in Fig. 5 to Fig. 9, the attitude constraints can be satisfied with UAS-BSMC method. And the harmful overshoots can be removed by the designed positively invariant sets. Therefore, we know that the proposed robust UAS-SMC control scheme can efficiently track the desired trajectories with attitude constraints.

5. Summary

In this article, a robust UAS-BSMC control scheme has been proposed for HSV with the attitude constraints. Rigorous analysis has been given for the convergence of all closed-loop signals under the proposed control schemes. Simulation results show the effectiveness of the robust UAS-BSMC scheme for the NSV. External disturbances may cause a system crash (e.g., Chen Q et al., 2018), in the following study, the robust attitude control scheme can be further developed for the HSV with disturbances and time-varying attitude constraints.

Acknowledgements

This work was supported by the National Natural Science Foundation of China [61603191], [61603189], China Postdoctoral Science Foundation [2018M630424], Science Foundation of State Key[614260403010117], Jiangsu Province Postdoctoral Fund [1401023C]. The authors also gratefully acknowledge the helpful comments and suggestions of the reviewers, which have improved the presentation.

References

[1] Shao X, Wang H. 2016. Back-stepping robust trajectory linearization control for hypersonic reentry vehicle via novel tracking differentiator. J. Journal of the Franklin Institute, 353(9), 1957-1984.

[2] Zhang Y, Yao Z, Yao Z, et al. 2016. An analysis of the stability and chattering reduction of high-order sliding mode tracking control for a hypersonic vehicle. J. Information Sciences, 348, 25-48.

[3] Bu X, Wu X, Wei D, et al. 2016. Neural-approximation-based robust adaptive control of flexible air-breathing hypersonic vehicles with parametric uncertainties and control input constraints. J. Information Sciences, 346, 29-43.

[4] Xu B, Guo Y, Yuan Y, et al. 2016. Fault-tolerant control using command-filtered adaptive back-stepping technique: Application to hypersonic longitudinal flight dynamics. J. International Journal of Adaptive Control & Signal Processing, 30(4):553-577.

[5] Y. Zhu, H. Su, and M. Krstic, 2015. Adaptive back-stepping control of uncertain linear systems under unknown actuator delay, Automatica,54: 256-265.

[6] Yin C, Hu B and Cheng Y. 2018. Design of fractional-order back-stepping sliding mode controller for the quadrotor unmanned aerial vehicles ,2017 36th Chinese Control Conference (CCC),Wuhan, 697-702.

[7] Shengli Shi, Mengting Liu, Jiayu Ma. 2018. Fractional-Order Sliding Mode Control for a Class of Nonlinear Systems via Nonlinear Disturbance Observer. J. International Journal of Applied Mathematics in Control Engineering, 1(1), 103-110.

[8] Yan Li and Ju-Beom Son, 2009. PMSM Speed Controller Using switching algorithm of PD and Sliding Mode Control, in CROS-SICE International Joint Conference, 1260–1266.

[9] Pukdeboon C. 2009. Optimal sliding mode controllers for attitude tracking of spacecraft, in Control Applications, (CCA) & Intelligent Control, (ISIC), 1708–1713.

[10] Xiaoyuan Luo, Shangbo Ge, Jiange Wang , Xinping Guan. 2018. Time Delay Estimation-based Adaptive Sliding-Mode Control for Nonholonomic Mobile Robots. J. International Journal of Applied Mathematics in Control Engineering, 1(1), 1-8.

[11] Polyakov, A., Poznyak, A. 2011. Invariant ellipsoid method for minimization of unmatched disturbances effects in sliding mode control. Automatica, 47(7), 1450-1454.

[12] Davila, J., Poznyak, A. 2011. Sliding mode parameter adjustment for perturbed linear systems with actuators via invariant ellipsoid method. J. International Journal of Robust and Nonlinear Control, 21(5), 473-487.

[13] Richter, H., O'Dell, B. D., Misawa, E. A. 2007. Robust positively invariant cylinders in constrained variable structure control. IEEE Transactions on Automatic Control, 52(11), 2058-2069.

[14] Pastravanu, O., Matcovschi, M. H. 2010. Linear time-variant systems: Lyapunov functions and invariant sets defined by Hölder

[15] Zipeng Han. 2014. Exterior Ballistics of Projectiles and Rockets .M. Beijing Institute of Technology Press

[16] Walton J. 1989. Performance sensitivity of hypersonic vehicles to changes of angle of attack and dynamic pressure, Cleveland, OH, USA, AIAA 89-2463,

[17] Fu J. 2013. Robust sliding mode control for near space vehicle. Ph.D. Nanjing University of Aeronautics and Astronautics, 35–37.

[18] Blanchini F. 1999. Set invariance in control. Automatica 35: 1747–1767.

[19] Qiang Chen, Yinqiang Wang, Zhongjun Hu. 2018. Finite Time Synergetic Control for Quadrotor UAV with Disturbance Compensation. J. International Journal of Applied Mathematics in Control Engineering, 1(1), 31-38.

Zhihao Yang is a second-year graduate student at School of Energy and Power Engineering, Nanjing University of Sciences and Technology. He obtained his B.E. degree from Nanjing University of Sciences and Technology in 2017. His main research interests are in the areas of nonlinear control and control applications.

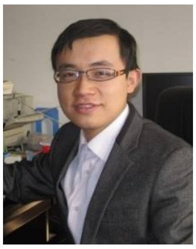

Jian Fu received his Ph.D. degree in control theory and control engineering from Nanjing University of Aeronautics and Astronautics. In the same year, he taught at Nanjing University of Science and Technology. Now, he is an associate researcher at NUST. He mainly engaged in nonlinear control, robust control, sliding mode control, adaptive observer design and so on.

Liangming Wang is a professor at School of Energy and Power Engineering, Nanjing University of Sciences and Technology. He received the Ph.D. degree in external ballistic engineering from Nanjing University of Sciences and Technology. His research interest covers Aircraft guidance and control technology, dynamic system modeling and algorithm research and so on.

Zhi Chen is a postdoctor at the School of Mechatronic Engineering and Automation, Shanghai University. He received his Master and PhD degree from Nanjing University of Aeronautics and Astronautics in 2011 and 2017. His research interest covers sliding mode variable structure control, robot control, flight control and simulation.

Hongyang Bai is an associate professor at School of Energy and Power Engineering, Nanjing University of Science and Technology. He received his PhD degree in navigation, guidance and control from Nanjing University of Science and Technology in 2012. His research interests include guidance and control technology, artificial intelligence and so on.